

Estimation of the Acoustic Waste Energy Harvested from Diesel Single Cylinder Engine Exhaust System

Claudiu Golgot^a, Nicolae Filip^b and Lucian Candale

Department of Automotive Engineering and Transport, Technical University of Cluj-Napoca, Romania

Keywords: Noise, Diesel, Acoustic, Energy Harvesting, FFT, Resonant Frequency.

Abstract: Noise generated in the operation of an internal combustion engine is an energy waste that produces noise pollution. Recovering some of this energy and transforming it into another form of usable energy brings significant benefits. We proposed to develop a device to recover this energy waste produced by the internal combustion engines, in the gases changing process. The developed energy recovery system is based on the Helmholtz resonator principle. For the conversion of acoustic waves into electricity, we used an audio speaker as a low-cost electromagnetic transducer located at the end of the resonant chamber. By audio playback of the acoustic signal recorded at the engine exhaust, we measured the electricity generated with the proposed recovery system. We found that the noise level measured at the exhaust depending on the engine speed range, follows a linear distribution law, instead, the harvested electric power varies nonlinearly. To find out the cause of the electric power variation, we performed a detailed FFT analysis. We found that at most engine speeds, the dominant amplitudes in the frequency spectrum are close to the resonant frequency of the system. With the proposed conversion system, we obtained a maximum value of the harvested electric power of 165 μ W.

1 INTRODUCTION

Road vehicles are generally recognized as a major source of urban noise pollution, mainly due to the noise produced by the exhaust system. Active methods to reduce exhaust noise and fuel consumption are proposed by Rossi and Cotana (Rossi et al., 2002). The studies were performed with an electromagnetic transducer for active noise control. Farid (Farid, 2015) presented a method of harvesting acoustic energy using an electromagnetic transducer based on the Helmholtz resonator principle. At the resonant frequency of 319 Hz, it obtained a maximum power of 789.65 μ W. Ming Yuan (Ming et al., 2018) using a similar device obtained a maximum power of 2.4 μ W.

Matova S.P. (Matova, 2010) uses a piezoelectric generator and an adjustable Helmholtz resonator to obtain energy from the air flow. Depending on the speed of the air flow, he adapted the Helmholtz resonator so that it has the same resonant frequency as the piezoelectric generator, obtaining a maximum electrical power of 2 μ W at an air flow of 13 m / s.

The conversion of acoustic energy is also found in research on thermo-acoustic generators, they transform thermal energy into acoustic energy and then into electricity using an acoustic-electric transducer.

Kees de Blok (Kees, 2010) obtained an efficiency of 8% with a generator composed of four thermo acoustic generators connected in series. Backhaus S.N. (Backhaus et al., 2012) presented an electric thermo-acoustic generator composed of a loop resonator tube using a low-cost commercial speaker as a linear alternator. It obtained, the maximum power of 11.58W from 703 W calorific power, an engine efficiency of 3.5%, an alternator efficiency of 46% and a generator efficiency of 1.65%.

Low-cost speaker efficiencies are mentioned by Zhibin Yu (Zhibin et al., 2010), he obtained an efficiency of 40% for a load close to the coil resistance. Bin Li (Bin et al., 2012) transformed the acoustic energy with a resonator tube and a piezoelectric rod mounted inside the tube. Thus, for a noise level of 110 dB it obtained a voltage of 15,689 V and a power of 12,397 mW. The amount of energy

^a <https://orcid.org/0000-0002-1890-8960>

^b <https://orcid.org/0000-0003-1342-2547>

obtained was based on the area and volume of the device used ($0.635 \text{ mW} / \text{cm}^2$ and $15.115 \text{ } \mu\text{W} / \text{cm}^3$).

In this paper we propose to use an electromagnetic transducer mounted in an acoustic system with Helmholtz resonator to convert into electricity some of the residual acoustic energy of the exhaust gases produced by a single-cylinder diesel engine.

2 MATERIALS AND METHODS

To recover the acoustic energy resulting from the evacuation of a diesel engine, we chose a system equipped with a Helmholtz resonator. This method provides a good response in a selective frequency band with a relatively accessible sizing (Martin et al., 2018).

Myonghyon (Myonghyon, 2008) showed that changing the dimensions not only changes the resonant frequency but also the amplitude pressure in the resonator cavity. We also considered the research on the reduction of acoustic energy and the influence of the Helmholtz resonator related by Ganghua Yu et al., (Ganghua et al., 2008).

The proposed system shown in Figure 1 composed of a main pipe through which the incident sound pressure wave (exhaust noise) evolves with a Helmholtz resonance chamber attached. The end of the resonant chamber in our case is elastic due to the membrane of the electromagnetic transducer (of the audio speaker).

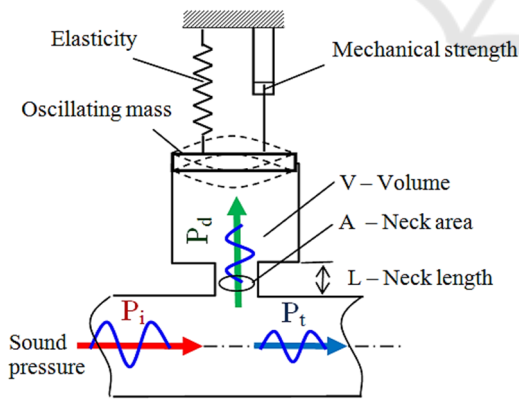


Figure 1: Helmholtz resonator of the conversion system where P_i – input pressure, P_d – dispersed pressure and P_t – transmitted pressure.

In this research, we also considered the volume changes of the Helmholtz cavity produced by the elastic movement of the audio speaker membrane under the action of the sound pressure wave. In the direction of propagation of the gas flow, at the end of

the pipe, we introduced an air filter to simulate the noise attenuator according to the engine architecture used in this research.

The acoustic conversion system (Figure 1) can be equated with an electrical circuit shown in Figure 2 where Z_i is the incident acoustic impedance (specific to the incident pressure wave in front of the resonator), Z_d represents the dissipated impedance of the resonator (resonant impedance) and Z_t is the transmitted impedance (after resonator).

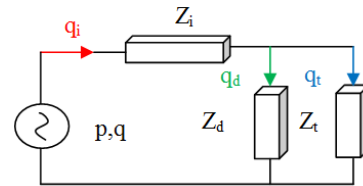


Figure 2: The equivalent electrical circuit of the conversion system.

In the equivalent circuit, the acoustic analogies according to Kirchhoff's laws are respected (Nicolae et al., 2012), where the volumetric acoustic speed is analogous to the electric current and the acoustic pressure is analogous to the electric voltage, according to the equations:

$$p = q_d \cdot Z_t + (q_i + q_d) \cdot Z_i \quad (1)$$

$$q_i = v_d + v_t \quad (2)$$

$$q_d \cdot Z_d = q_t + Z_t \quad (3)$$

where q / q_i is initial volumetric acoustic speed, Z_i is acoustic impedance of the pipe before resonator, q_d is volumetric acoustic speed from resonator neck, Z_d is acoustic impedance of the Helmholtz resonator, q_t is volumetric acoustic speed in front of the resonator, Z_t is acoustic impedance of the piping after the resonator.

The resonator was dimensioned considering the range of diesel engine speeds and the mechanical resonance frequency of the electromagnetic transducer. Since we used a single-cylinder engine, in calculating the resonant frequency of the incident wave it was no longer necessary to consider the number of cylinders (Juan et al., 2017).

The resonant frequency of the Helmholtz system was calculated using Equation (4) (Brian et al., 2015; Nicolae, 2000) where c is the speed of sound, A is the area of the resonant neck section, l is the length of the resonant neck, and V is the volume of the resonant chamber,

$$f_0 = \frac{c}{2\pi} \cdot \sqrt{\frac{A}{l \cdot V}} \quad (4)$$

For the calculation of the resonance chamber volume, the fixed diameter of the electromagnetic transducer located at the end of the chamber was considered. The electromechanical transducer (audio speaker) mounted at the end of the resonant chamber (Table 1) is used in reverse function. It generates electricity due to the pulsations of the electromagnetic core resulting from variations in sound pressure.

Table 1: Technical data of the audio speaker.

Maximum load power	Moving mass of the speaker	Frequency range
$P_z=60$ [W]	$M_{ms}=13.18$ [g]	$f=50-7000$ [Hz]
Nominal power	Membrane surface	Impedance
$P_n=40$ [W]	$S_d=95$ [cm ²]	$Z=8$ [Ω]
Resonance frequency	Mechanical strength	Membrane elasticity
$f_r=54$ [Hz]	$R_{ms}=1.23$ [kg/s]	$C_{ms}=0.65$ [mm/N]

The diesel engine used in this research has the following technical parameters:

- vertical single-cylinder model, four-stroke, air-cooled, direct injection;
- 86 mm bore, 72 mm stroke;
- maximum power 5.7 kW, speed 3000 rpm;
- nominal speed 2880 rpm.

The components of the conversion system are shown in Figure 3.

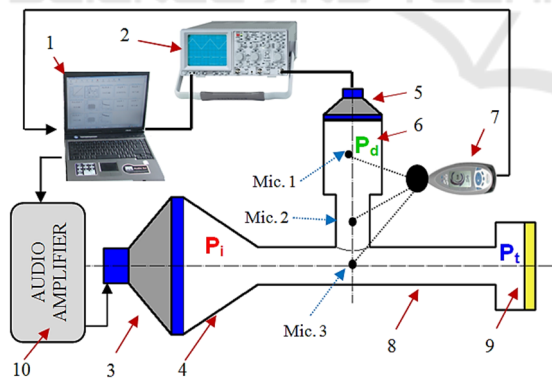


Figure 3: Experiment setup for evaluating the acoustic energy conversion where 1 – laptop, 2 – oscilloscope, 3 – audio speaker, 4 – metal cone, 5 – electromagnetic transducer, 6 – Helmholtz resonator, 7 – sound level meter, 8 – metal pipe, 9 – anechoic material, 10 – audio signal amplifier, Mic. – piezoelectric microphone.

The proposed research method is performed in two stages. For data collection, in the first stage, noise measurements are performed. In the second stage, conversions and data processing are performed.

These research stages require separate laboratory stands. Figure 4 shows the block diagram and the sequence of stages of this research.

The first stage (noise measurements) involves recording the exhaust noise of the single-cylinder diesel engine for a speed range between 1500 rpm and 3200 rpm at-load free mode (Figure 5).

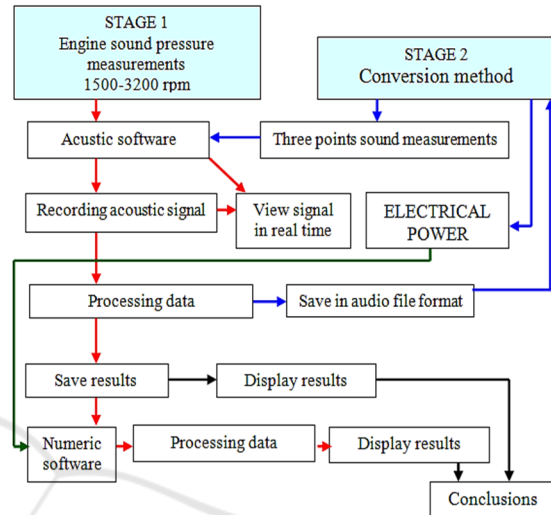


Figure 4: Methodological scheme of the experiment.

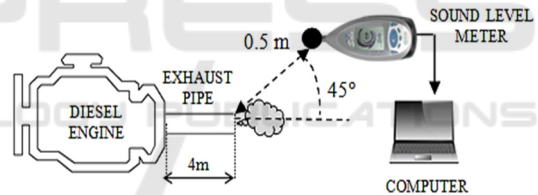


Figure 5: Sound pressure measurements at the end of the exhaust pipe.

Noise measurements are analysed in real time and they are processed by the software compatible with the sound level meters we used. These software’s allow the sampling of the acoustic signal with a period of three engine cycles and offering the possibility to save it in different file formats.

To calculate the required time of three engine cycles we used Equation (5), (Nicolae, 2000; Candale, 2013),

$$\Delta_t = \frac{k}{\frac{n}{60} \cdot \frac{2}{\delta}} \quad (5)$$

where Δ_t – time sampling, k – number of complete engine cycles (in our case three), δ – number of engine strokes (in our case four) and n – operating engine speed (rpm).

To determine the corresponding number of values (x data units) of three engine cycles in the whole string of values we used the equation:

$$x = \Delta_t \cdot f_{\text{acquisition}} \quad (6)$$

where $f_{\text{acquisition}}$ is the acquisition frequency of the sound level meter (51,200 x/ sec).

In second stage for signal processing, the conversion of the recorded exhaust noise in audio format file ("waveform audio file") was performed. By playing in the conversion system the audio files containing the noise produced by the engine for each engine speed range the resulting electric power is measured.

The sound pressure level from the conversion system is measured in three points. The first microphone is placed in the resonator chamber (Mic. 1), the second microphone is mounted in the neck of the resonator (Mic. 2) and the third microphone (Mic. 3) is placed in front of the resonator (Figure 3).

All measurements are again processed and analysed within the software programs we used. In the end of the research, we obtained results like:

- sound pressure level of the exhaust noise depending on engine speed;
- sound pressure level measured in the conversion system;
- electrical intensity and voltage generated by the electromagnetic transducer;
- electric power depending on the sound pressure level and engine speed;
- dominant amplitudes in FFT frequencies (Fast Fourier Transform).

The frequency at which the system begins to vibrate (resonates) under the action of an external energy source is also called the resonant frequency. The resonant frequency depends on the system characteristics such as density, rigidity, mass, dimensions, materials, etc. Several experimental tests are performed to determine the resonant frequency of the conversion system.

By laboratory tests, the resonant frequency of the conversion system was determined. Through acoustic software (tone generator software), sounds with frequencies between 40 Hz and 200 Hz were played through the audio speaker. The frequency of the sound played in the system was increased by a step of 10 Hz.

Each sound played in the system was increased using an audio amplifier to ensure an SPL of 120 dB (sound pressure level) equivalent to SPL_{MAX} (maximum sound pressure level) of the measured exhaust noise. These tests are performed by positioning the electromagnetic transducer in the

resonance chamber at different distances from the Helmholtz resonator neck (0.2 m to 0.3 m) shown in Figure 6.

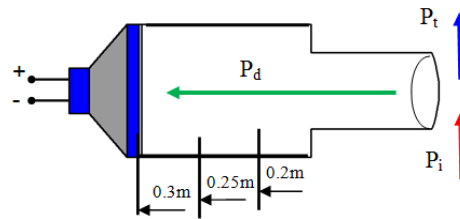


Figure 6: Electromagnetic transducer position in the resonance chamber where P_i – input pressure, P_d – dispersed pressure and P_t – transmitted pressure.

By playing in the system pure sounds with different frequencies (keeping the frequency step of 10 Hz) we found that its resonant frequency changes with the transducer position. If the transducer is positioned closer to the resonator's neck, the resonant acoustic frequency increases.

By measuring the electrical voltage generated by the electromagnetic transducer, the frequency where we obtained the highest value of electrical voltage was established. This frequency is corresponding to the resonant frequency of the conversion system (Minu, 2015). We found that at a frequency of 160 Hz a voltage of 434 mV and a current of 27.9 mA is generated given that the mechanical resonance frequency of the electromagnetic transducer is 54 Hz, shown in Figure 7 and Figure 8.

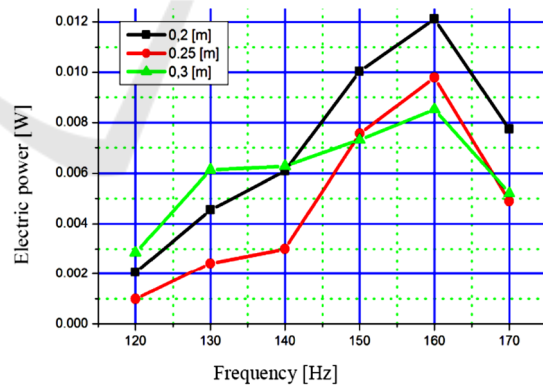


Figure 7: Electrical power generated with the conversion system for the frequency range of 120 Hz and 170 Hz with the position of the electromagnetic transducer at 0.2 m, 0.25 m and 0.3 m.

At the frequency of 160 Hz and 0.2 m from the electromagnetic transducer to the resonator neck, the generated electric power has the maximum value. Figure 9 and Table 2 shows the variations of the electric current with an amperage between 11.6 mA –

27.9 mA and the electric voltage between 178 mV – 434 mV.

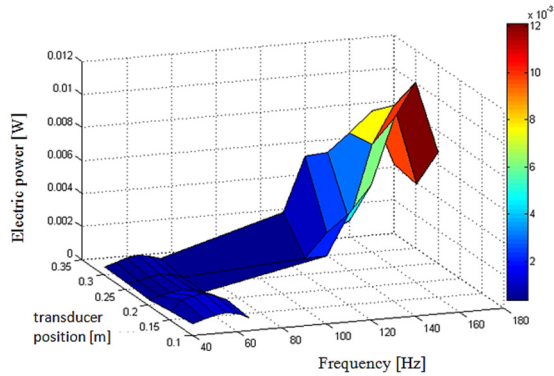


Figure 8: 3D representation of the electrical power generated depending on the position of the transducer (0.1 m – 0.3 m) and frequency range of 40 Hz and 180 Hz.

Table 2: The resulting voltage and the electrical intensity depending on the sound frequency with the electromagnetic transducer mounted at 0.2 m from the resonator neck.

Frequency [Hz]	Electrical intensity [mA]	Electric voltage [mV]
120	11.6	178
130	17.1	266
140	19.8	308
150	25.4	395
160	27.9	434
170	22.3	347

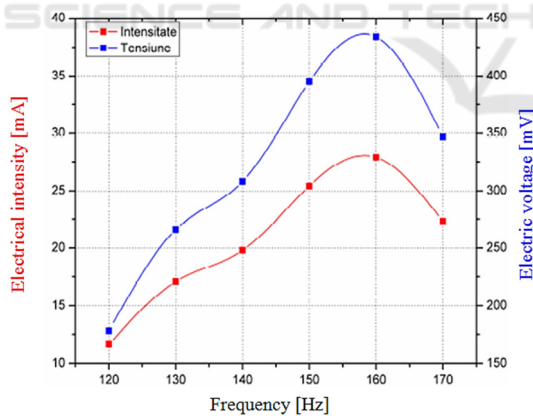


Figure 9: Graphical representation of the resulting voltage and electrical intensity with the electromagnetic transducer mounted at 0.2 m from the resonator neck.

The graph of the electrical power obtained in the frequency range of 110 Hz and 170 Hz is presented in Figure 10. Following the results, the resonant frequency of the conversion system at 160 Hz can be confirmed.

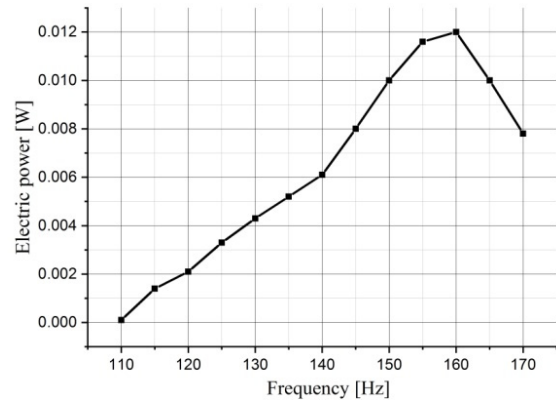


Figure 10: The electrical power generated by the conversion system with the electromagnetic transducer mounted at 0.2 m from the resonator neck.

3 RESULTS

3.1 Sound Pressure Level and Electrical Power

The sound pressure measured at the outlet of the diesel engine is processed for the period of three engine cycles in the speed range between of 1500 rpm and 3200 rpm, at-load free mode. The recorded sound pressure values are shown in Figure 11.

It can be seen how the sound pressure follows the same law of variation for each engine cycle performed. The maximum measured pressure is between 5 Pa and 100 Pa increasing with the engine speed. The time required to perform three engine cycles decreases with increasing engine speed and it is between 0.25 and 0.12 seconds.

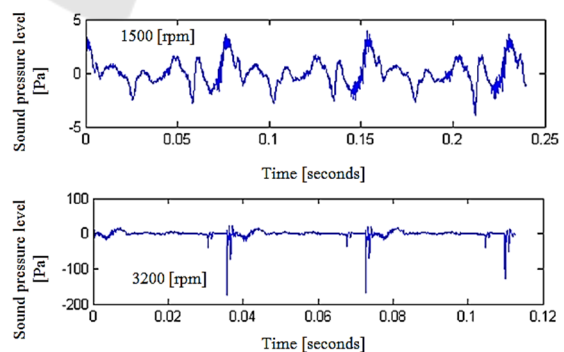


Figure 11: Sound pressure level recorded for the speed range of 1500 rpm and 3200 rpm.

By audio playback of the noise produced by the engine in the conversion system, the variation of the acoustic pressure for each speed range can be

observed in Figure 12. The variation of the acoustic pressure in the system influences the sensitivity of the electromagnetic transducer by the amount of electricity generated by it.

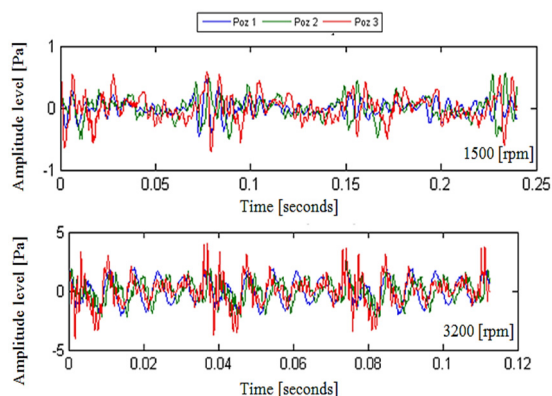


Figure 12: The acoustic pressure recorded for the three point's measurements in the conversion system for 1500 and 3200 rpm speed range (poz 1 – Mic.1, poz 2 – Mic.2 and poz 3 – Mic.3).

Figure 13 shows the difference between the noise level measured physically at the engine exhaust (Lp) and the noise level measured in the conversion system through the three points depending on the diesel engine speed.

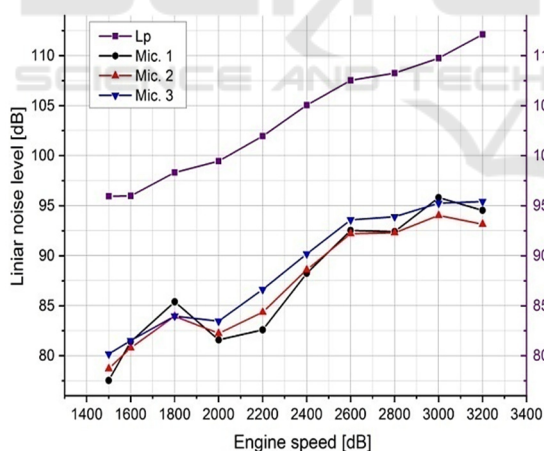


Figure 13: The difference between the noise level measured at the engine exhaust system (Lp) and the noise level measured in the conversion system.

The experimental results show that the sound pressure measured in the conversion system is much lower (1 – 5 Pa) than the sound pressure measured directly at the engine outlet although the audio amplifier operates at maximum capacity. The highest value of sound pressure was recorded at the microphone 3 (Mic.3) positioned in front of the

Helmholtz resonator because it is the closest point to the audio speaker that generates the noise in the conversion system.

From the graph of the generated electric power (Figure 14) we found that its value does not comply with the same law of linear distribution as the noise level, there are speeds (2800 rpm – 3200 rpm) where the measured electric power decreases.

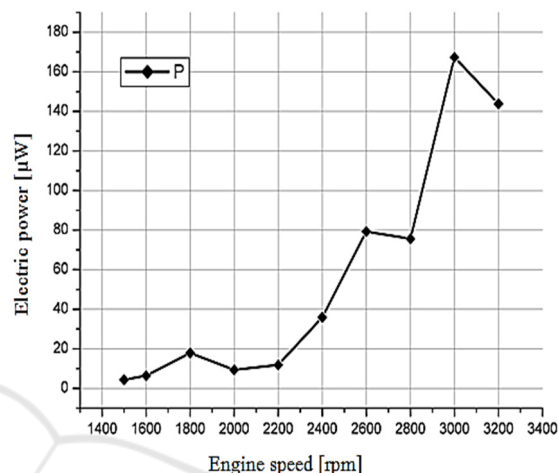


Figure 14: Graph of electric power harvested according to engine speed.

To find out the cause of this difference we performed an FFT analysis calculation (Fast Fourier Format).

3.2 Detailed FFT Analysis

The detailed FFT analysis was performed to find the cause of variations in electrical power and to determine the dominant amplitudes and their frequency in terms of frequency spectrum.

Figure 15 shows the FFT analysis of the noise recorded at the engine exhaust depending on the engine speed.

The data values resulting from the FFT analysis are presented in Table 3 as follows:

- the value of the dominant amplitude, the amplitude with the closest frequency to the resonant frequency of the conversion system (160 Hz);
- the sound pressure level of the maximum amplitude from the total frequency spectrum;
- the frequency of the maximum amplitude, corresponding to the operating speed of the combustion engine.

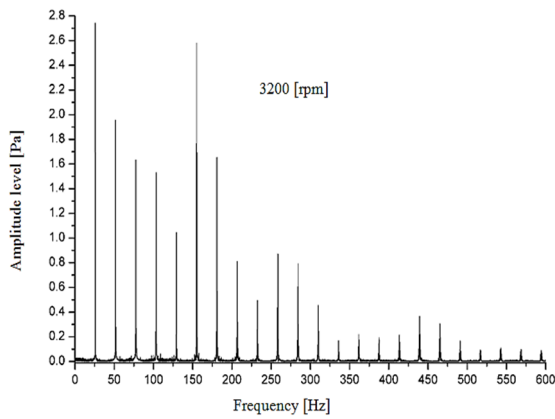


Figure 15: Exemplification of FFT analysis in the low frequency range of the acoustic signal measured at the engine exhaust for the speed range 3200 rpm.

Table 3: Data extracted from the FFT analysis of the acoustic signals recorded at the engine exhaust.

Engine speed [rpm]	Dominant pressure amplitudes [Pa]	Maximum pressure amplitude [Pa]	Frequency of maximum amplitude [Hz]
1500	0,05	0,50	23
1600	0,12	0,40	23
1800	0,30	0,56	16
2000	0,21	0,83	18
2200	0,17	1,72	19
2400	0,42	2,00	20
2600	1,05	2,17	42
2800	1,25	2,95	25
3000	2,60	2,75	25
3200	1,75	2,75	25

From the obtained values it can be observed how at most speeds, the frequency of the maximum amplitude belongs to the low frequency domain with values below 25 Hz. An exception occurs at the speed of 2600 rpm where the frequency of the maximum amplitude is 42 Hz. This frequency is the closest to the mechanical resonance frequency of the low-cost transducer (54 Hz).

From the graphical representation of the maximum amplitude of the sound pressure and the engine speed, we can observe how the amount of recovered electricity depends on the intensity of the amplitudes closest to the resonant frequency of the system.

Comparing the maximum amplitudes (Figure 16.a) with the graph of the measured electric power (Figure 16.b), we found that the frequency of the dominant amplitude is found around the resonant frequency of the system. Due to this, the energy recovered from the system does not comply with the same law of variation valid for engine speeds.

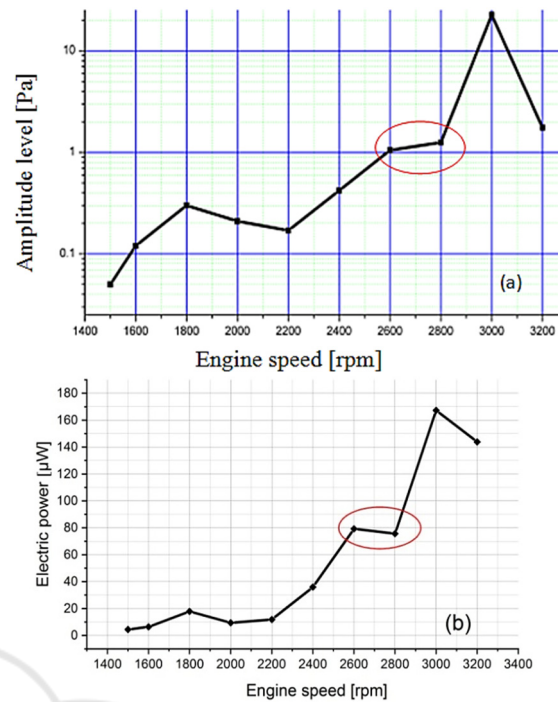


Figure 16: The variation graphs of (a) the dominant amplitudes found closest to the resonant frequency of the conversion system compared to (b) the electric power (P) generated by the system.

From the analysis regarding the maximum sound pressure level measured at the engine exhaust for each engine speed (Figure 17), it can be seen how it increases linearly with the engine speed.

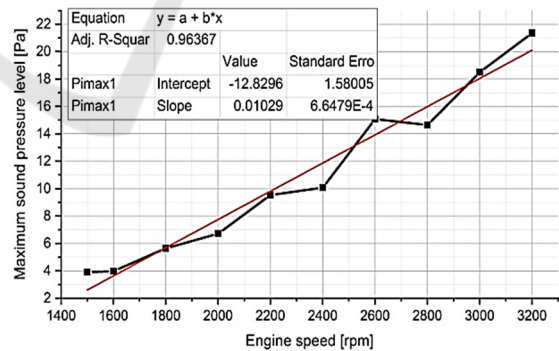


Figure 17: Variation of the maximum sound pressure level of the noise recorded at the engine exhaust for each operating speed and linear interpolation.

From the analysis of the noise level measured in the three positions of the system (Figure 18), it can be seen how the highest sound pressure level was measured in the positions of microphones 3 and 2 (closest to the noise source).

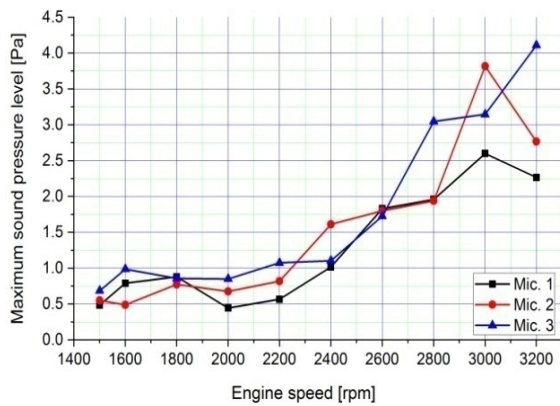


Figure 18: Variation of the maximum sound pressure level of the noise recorded at the engine exhaust for each operating speed and linear interpolation.

The maximum sound pressures level for the three positions measurements are represented by linear and exponential interpolation in Figure 19, Figure 20 and Figure 21.

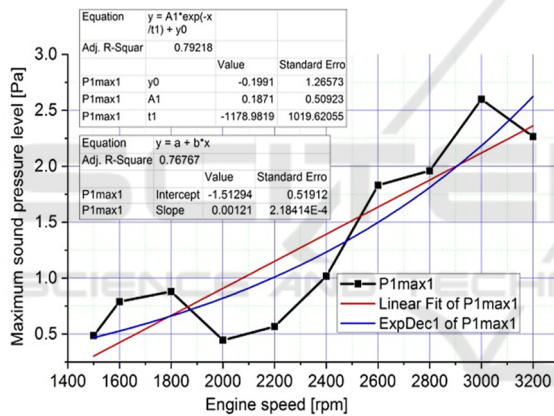


Figure 19: Linear and exponential interpolation of the noise measured in point 1 (Mic.1) of the conversion system for each engine speed.

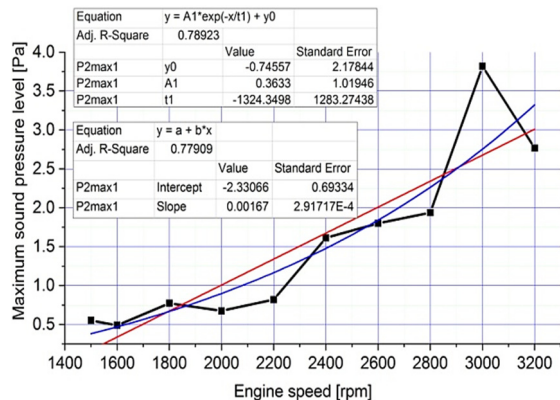


Figure 20: Linear and exponential interpolation of the noise measured in point 2 (Mic.2) of the conversion system for each engine speed.

From these representations, only in the case of the acoustic pressure measured by the microphone 3 (Figure 21), it can be said that its variation respects a law of exponential growth with the increase of the speed.

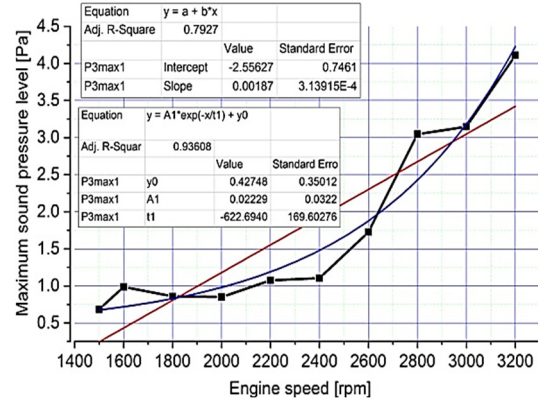


Figure 21: Linear and exponential interpolation of the noise measured in point 3 (Mic.3) of the conversion system for each engine speed.

The recovered power values in the system are represented by linear and exponential interpolation in Figure 22. Also, in this case the variation law respects an exponential growth depending on the engine speed.

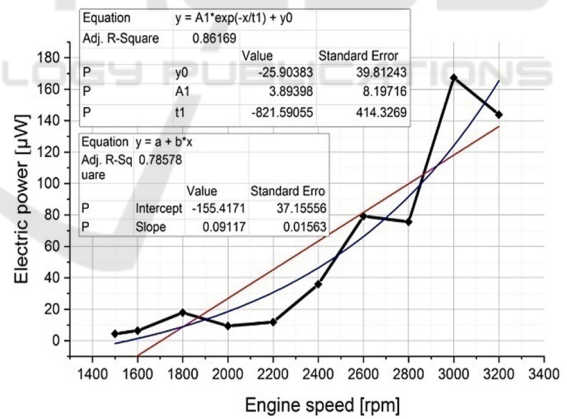


Figure 22: Linear and exponential interpolation of recovered electrical power with the conversion system.

4 CONCLUSIONS

At the end of our research and experiments, the proposed conversion system works but the amount of electricity generated is low (165 µW).

Compared to other research methods in the field of residual acoustic energy harvesting, the maximum energy value was obtained using thermoacoustic

transducers with a power of 11.58W (Backhaus et al., 2012), piezoelectric transducers 12.397 mW (Bin et al., 2012) followed by electromagnetic transducers 789, 65 μ W (Farid, 2015) and 2.4 μ W (Ming et al., 2018).

Helmholtz type resonators are mainly influenced by the resonant frequency. One possible reason for the low harvested electrical power is the low value of the resonant frequency of the conversion system (160 Hz). This is due to elements such as the large diameter of the audio speaker (130 mm) influencing the dimensions of the resonant chamber, the rigidity of the elastic membrane, the mass of the oscillating system and the density of the materials used.

Research in the field has concluded that with the increase of the resonant frequency of this type of recovery system, the harvested electrical power also increases. The resonance frequency can be increased by choosing a more sensitive electromagnetic transducer with a very elastic membrane, an oscillating mechanism with a lower weight, reducing the volume in the resonance chamber and positioning the transducer as close as possible to the noise source.

Another possible reason may be that the noise on the engine exhaust system piping is in the form of plane sound waves and the noise measured at the outlet propagates in the form of spherical waves. The amplitude of the spherical sound pressure wave decreases with distance.

Given that the reproduction of sound (by audio playback) in the conversion system was achieved at a much lower level compared to the sound pressure level physically measured at the exhaust of the single-cylinder diesel engine, the amount of energy that could be converted directly from the exhaust system of the engine would be proportionately bigger.

Also, noise level in the exhaust pipe is bigger than the noise level measured at 0.5 m from the end of the pipe and at an angle of 45° to the axis of the pipe (Figure 5) and therefore the conversion potential is higher.

From (Figure 9) and (Figure 10) we can see that the collected power is higher when the noise level increases and when the acoustic wave form is close to the sensibility of the traducer near to the resonant frequency of the conversion system.

The proposed conversion system, equipped with a Helmholtz resonator, works by harvesting low power energy. The electricity generated depends on the operating speed of the engine this is explained by the increase in the noise level as the engine speed increases.

The biggest challenges for continuing this research are increasing the resonance frequency,

increasing the electrical power and finding a storage method for later use. Also, the proposed conversion system can be developed through noise reduction research at the intake and exhaust system of internal combustion engines. In this case the high temperature of the exhaust gases requires the selection of some transducers with high temperature resistance.

REFERENCES

- Cotana, F., Rossi, F., Buratti, C., 2002. Active noise control technique for diesel train locomotor exhaust noise abatement. In *144th meeting of the Acoustical Society of America*. Cancun, Mexico, pp. 1-7.
- Backhaus, S., Yu, Z., Jaworski, A.J., 2012. Travelling-wave thermo-acoustic electricity generator using an ultracompliant alternator for utilization of low-grade thermal energy. In *Applied Energy*. pp. 135-145.
- Bin, L., Andrew, J., Jeong, H.Y., 2012. Acoustic energy harvesting using quarter-wavelength straight-tube resonator. In *ASME, International Mechanical Engineering Congress & Exposition*. Houston, Texas, USA, pp. 467-473.
- Brian, C., Jordan, M., William, W., et. al., 2015. Experimental realization of extraordinary acoustic transmission using Helmholtz resonators. In *AIP Advances* 5.
- Candale, L., 2013. Research on the recovery of acoustic energy from vehicle noise and the conversion into electricity. In *PhD Thesis*. Tech. Univ. of Cluj-Napoca, 157-181.
- Farid, U.K., 2015. Electromagnetic energy harvester for harvesting acoustic energy. In *Indian Academy of Sciences*. Pakistan, volume 41, pp. 397-405.
- Filip, N., 2000. *Vehicle noise*, Publishing House Todeco. Cluj-Napoca, Romania.
- Filip, N., Fodor, G., Candale, L., 2012. Estimation of acoustic energy harvested from sound using electromagnetic transducer. In *New Trends and Perspectives, 15th International Conference on Experimental Mechanics*. Porto, Portugal, pp. 555-557.
- Ganghua, Y., Deyu, L., Cheng, L., 2008. Effect of internal resistance of a Helmholtz resonator on acoustic energy reduction in enclosures. In *The Journal of the Acoustical Society of America*. volume 124, pp. 3534- 3543.
- Juan, L., Yifeng, L., et. al., 2017. Manipulation of acoustic wavefront by gradient metasurface based on Helmholtz Resonators. In *Scientific Reports*, Nature.
- Kees de Blok, 2010. Novel four-stage travelling wave thermoacoustic power generator. In *ASME, 3th Joint US-European Fluids Engineering Summer Meeting with 8th International Conference on Nano-channels, Micro-channels and Mini-channels*. Montreal, Canada, pp. 73-79.
- Martin, D., Michael, K., Echart, K., et al., 2018. Experimental Study of Advanced Helmholtz Resonator Liners with Increased Acoustic Performance by Utilising Material Damping Effects. In *Applied Sciences*. volume 8, pp. 1-18.
- Matova, S.P., 2010. Harvesting energy from airflow with micro-machined piezoelectric harvester inside a

- Helmholtz resonator. In *Proc. Power MEMS*. Leuven, Belgium, pp. 183-186.
- Ming, Y., Xiaohui, W., Zhenjun, D., 2018. Low frequency acoustic energy harvesting adopting slit Helmholtz resonator. In *Vibroengineering Procedia*. volume 20, Nanjing, China, pp. 151-155.
- Minu, A., Ezhilarasi, D., 2015. Improved acoustic energy harvester using tapered neck Helmholtz resonator and piezoelectric cantilever undergoing concurrent bending and twisting. In *ICOVP, 12th International Conference on Vibration Problems*. Tamilnadu, India, pp. 674-681.
- Myonghyon, H., 2008. Sound reduction by a Helmholtz resonator. In *PhD Thesis*. The department of Mechanical Engineering and Mechanics, Lehigh University, pp. 33-48.
- Zhibin, Y., Arthur, J., 2010. Design of a low-cost thermo-acoustic electricity generator and its experimental verification. In *10th Biennial Conference on Engineering Systems Design and Analysis*. Istanbul, Turkey, pp. 191-199.
- Diesel Engine Service Manual, KM186FA, Available online: www.link.com (last access: 06.09.2020).
- User manual, Handbook of 01dB Software. Vibrotest, DBFA - NetdB12, Software Version 4.801.

